Shahrood University of Technology

Journal of Mining and Environment (JME)

Journal homepage: www.jme.shahroodut.ac.ir

Iranian Society of Mining Engineering (IRSME)

Analysis of Grain Size Effect on Mechanical Properties of Sandstone with Experimental and Numerical Methods

Enayatallah Emami Meybodi*, and Fatemeh Taajobian

Department of Geology, Yazd University, Yazd, Iran

Article Info

Received 29 March 2023
Received in Revised form 22 April 2023
Accepted 5 May 2023
Published online 5 May 2023

DOI:10.22044/jme.2023.12892.2339

Keywords

Grain Size
Sandstone
PFC2D
Distinct Element Method
Mechanical Properties

Abstract

Due to the challenge of finding identical rock samples with varying grain sizes, investigating the impact of texture on rock material has been given less attention. However, macroscopic properties such as compressive strength, tensile strength, and modulus of elasticity can indicate microscopic properties like intergranular resistance properties influence rock fracture toughness. In this work, both the experimental and numerical methods are used to examine the effect of grain size on the mechanical properties of sandstone. Uniaxial compressive strength and indirect tensile tests are conducted on sandstone samples with varying grain sizes, and the particle flow code software is used to model the impact of grain dimensions on intergranular properties. Flat joint model is applied for numerical modeling in the particle flow code© software. The aim of this work is to validate the numerical model by peak strength failure and stress-strain curves to determine the effect of grain size on the mechanical behavior. The results show that increasing grain size significantly decrease compressive strength, tensile strength, and modulus of elasticity. The impact of the change in grain size is more significant on compressive strength than on the other two properties. The correlation coefficient for tensile strength and grain size is R2 = 0.57, while for modulus of elasticity and grain size, it is R2 = 0.79. The PFC software helps calibrate intergranular properties, and investigate the effect of changing grain size on these properties. Overall, this study offers valuable insights into the relationship between the grain size and the mechanical properties of sandstone, which can be useful in various engineering applications, especially in petroleum geo-mechanics.

1. Introduction

The texture of sandstone plays a crucial role in various engineering projects such as petroleum geo-mechanics, rock mechanics, and environmental engineering. Understanding the variations in sandstone texture is essential in designing and optimizing these projects to achieve the desired outcomes [1]. Sandstones show a great deal of variation in mineral composition, and degree of sorting due to their different environment of formation such as rivers sand deposit, and wind sand piles up [2]. The strength and deformation characteristic of rock is a fundamental topic of great interest to engineers in rock mechanics [3]. A proper estimation of rock strength and deformation parameters is important for stability evaluation of structures in many rock engineering applications such as slopes, deep tunnels, boreholes, underground caverns, dams, wells, and foundations [4].

Golewski [5] and Golewski and Szostak [6] investigated the use of nano-silica and coal fly ash (CFA) in cement concrete mix to improve its mechanical parameters and micro-structure. The results show that the combination of 5% nano-silica and 15% CFA had the greatest improvement in compressive and splitting tensile strength, making it an eco-friendly alternative for producing stronger concrete composites. Golewski [7] investigation of the fracture mechanics parameters of concretes made with quaternary binders, using a combination of fly ash, silica fume, and nano-silica as a partial replacement for ordinary Portland

✉ *Corresponding author: en.emami@yazd.ac.ir (E. Emami Meybodi)*

cement, found that the optimal mixture contained 80% OPC, 5% FA, 10% SF, and 5% nS, while concrete with higher content of FA additive had the worst parameters.

With the rapid development of infrastructure construction, a considerable number of rock engineering's have appeared. To ensure the stability and safety of rock engineering, it is quite important to study the mechanical properties of different kinds of rocks. Rocks are natural geological materials that have many internal joints, fractures, and cavities. Due to these flaws, the mechanical properties of rocks are extremely complicated [8]. To meet the need of rock engineering construction, the researchers have performed many studies on the stress–strain behaviors and constitutive relations of rocks. A laboratory test is the most direct and effective method to observe rock mechanical behaviors [9]. Utili and Nova [10] conducted a study on the Discrete Element Method (DEM) analysis of bonded granular geo-materials. This study used the PFC software to simulate the behavior of bonded granular materials under various loading conditions. The study found that the strength and deformation behavior of the materials were influenced by the particle size distribution. Ding *et al*. [11] investigated the effect of model scale and particle size distribution on PFC3D simulation results. The study found that the results of PFC simulations were sensitive to the particle size distribution, and that increasing the number of particles in the model improved the accuracy of the simulation.

Nemat-Nasser [12] used the PFC software to simulate the deformation and failure of rock specimens under uniaxial compression. The specimens had different grain sizes, ranging from 0.4 mm to 4 mm. The study showed that the strength of the specimens decreased as the grain size increased. They attributed this behavior to the fact that larger grains have higher porosity and more flaws, which makes them more prone to failure. Külekçi, *et al*. [13] determined that the rock mass should be blasted for loosening before being dug with hydraulic breakers, and identified load strength index, geological strength index, and rock mass weathering as the most suitable parameters for surface excavational classification. The Kulekci *et al*. [14] study successfully obtained recycled aggregates (RA) from construction debris and demonstrated that RA can be used as a sustainable alternative to natural aggregates in various applications such as in concrete aggregate, underground filling in mining, filling material in gunned concrete, and filling materials on highways.

The mechanical behavior of red sandstone was experimentally studied under different confining pressures. On fault breccia specimens, the triaxial compression tests were conducted and analyzed the influencing factors on their compressive strength [15]. Amann *et al*. [16] investigated the mechanical behavior of clay shale and proposed an S-shaped failure criterion to describe their experimental data. Zhang *et al*. [17] carried out triaxial compression experiments on cataclastic sandstone specimens to investigate their failure process, finding the strain–stress curves of cataclastic sandstone. By Cundall *et al*. [18], a synthetic particle flow code model was used in the Lac du Bonnet Granite rock sample to reproduce crack initiation stress. Hazzard and Young [19] developed a technique to dynamically quantify AE in a PFC model. Fakhimi *et al*. [20] indicated that the numerical model of PFC2D was able to reproduce the damaged areas observed in laboratory tests. Diederichs [21] used PFC for the macroscopically tensile and compressive state to analyze tensile damage characteristics at the grain scale. Hazzard and Young [22] PFC3D was proposed for 3D simulations of acoustic activity. Fakhimi *et al*. [23] studied the damage zone or shear band in rock through numerical and physical experiments. The Wanne and Young [24] numerical studies were carried out on thermally-induced fracturing around openings in granite. Zhao [25] studied the mechanism of the failure process in rocks such as the initiation, and propagation of cracks from pre-existing flaws has been analyzed using BPM. Khazaei *et al*. [26] analyzed the fracturing process in the intact rock through the acoustic emission energies using numerical model simulation with PFC3D. Ozturk and Altinpinar [27] used the uniaxial compressive strength tests and point load tests were performed on trona and interbed of volcano-sedimentary rock, and a numerical model developed using the distinct element method (DEM) in the particle flow code (PFC) software.

He and Afolagboye [28] constructed a numerical model using the distinct element method (DEM) in particle flow code to understand the effect of lamination on the anisotropic behavior of shale. Yin and Yang [29], simulated the mechanical behavior of artificial transversely isotropic rock under uniaxial compression. In their respective works, Zhou *et al*. [30] employed the flat joint model (FJM) and the smooth joint model (SJM) to simulate the shale matrix and layer planes, while Bahaaddini *et al*. [31] studied the effects of joint

geometrical parameters on the uniaxial compressive strength (UCS) and deformation modulus, Zhao *et al*. [32] investigated the deformation and failure modes of a rock mass containing different numbers of concentrated parallel joints at varying spacing, while Huang *et al*. [33] studied the effects of micro-parameters of SJM on the macro-properties of rocks under uniaxial compression, while Wang *et al*. [34] developed a model to simulate strength variations for anisotropic rock masses under uniaxial compression.

Chong *et al*. [35] performed a numerical investigation of bedding plane parameters of transversely isotropic shale, and in another work, Chong *et al*. [36] studied the effects of layer orientation on the mechanical behavior of shale, while *Huan et al*. [37] developed an SJM-based model to characterize the mechanical properties of transversely isotropic rock masses, and while Lei *et al*. [38] conducted experimental and numerical investigations on the meso-fracture mechanism of Longmaxi shale with varying crack-depth ratios. This study analyzed two samples of sandstone with different grain sizes. As intergranular properties cannot be measured in a lab, the samples were tested for uniaxial compressive strength, tensile strength, and modulus of elasticity using methods like the indirect tensile test. Numerical modeling was used to calibrate intergranular properties in a sample with coarse grains, and then the effect of changing grain dimensions was investigated by assuming the same intergranular properties.

2. Data Collection

2.1. Studied area

Yazd province is located in the middle of the central plateau of Iran. Central Iran is one of the main and major units that is located in the center of Iran in the form of a triangle and is considered to be the largest and most complex geological unit. The sub-continent of Central Iran is a part of Middle Iran that is surrounded by the Sistan, Nayin, Baft, Daroneh, and Kashmar-Sabzevar ophiolitic seams and can be divided into it is Lut Block, Shotori Horst, Tabas Graben, Kalmard Horst, Posht-e-Badam Block, Bayazeh-Bardsir Graben, and Yazd Block [39]. The studied area is located in Yazd block. The Yazd block is the western part of the central Iranian subcontinent, which is bounded by the Darone fault from the north and the Nain-Baft ophiolitic belt from the west [40].

In this study, sandstone samples were taken from two areas of Bidakhavid from the Sangestan Formation and Eslamiyeh from the Shemshak Formation in the Yazd province (Figure 1). The studied area is a part of the Uromieh-Dokhtar volcanic zone [41]. Based on research and field observations, the geological constituent units in the region include limestone, dolomite and dolomitized limestones of the Jamal Formation of Middle Permian age. The main part of the batholith is composed of granitoid rocks including granodiorite, monzo granite, Sino granite, and tonalite. The Shirkoh batholith has a wide time range of plutonism from the middle Jurassic to the post-Cretaceous [42, 43].

The Sangestan formation, which mostly consists of conglomerate-sandstone and arkose, covers the intrusive mass of Shirkoh with an angular variation. The gray colored limestones of the Taft formation of early Cretaceous age, which are located on the limestones of the Sangestan formation, cover the coarse-grained conglomerate of Kerman. The Eocene in this area mostly consists of andesitic, dacite and rhyodacite lavas along with tuffs and associated breccias covered by Oligocene and Quaternary rock units. The industrial soil of Bidakhavid mine is formed in the form of Quaternary alluvium in the fault pit. This mine is the result of the accumulation and decomposition of granite alluvial sediments; these sediments can be seen in various colors from creamy white to brown. Ferric oxide plays an important role in changing the color of the units, alteration has occurred on a very large scale in the region, the granularity of the altered units is mostly gravel, sand, and clay. According to the field evidence and the study of geological maps, the process of alteration and weathering has occurred in a fault pit that is related to the Quaternary period [44].

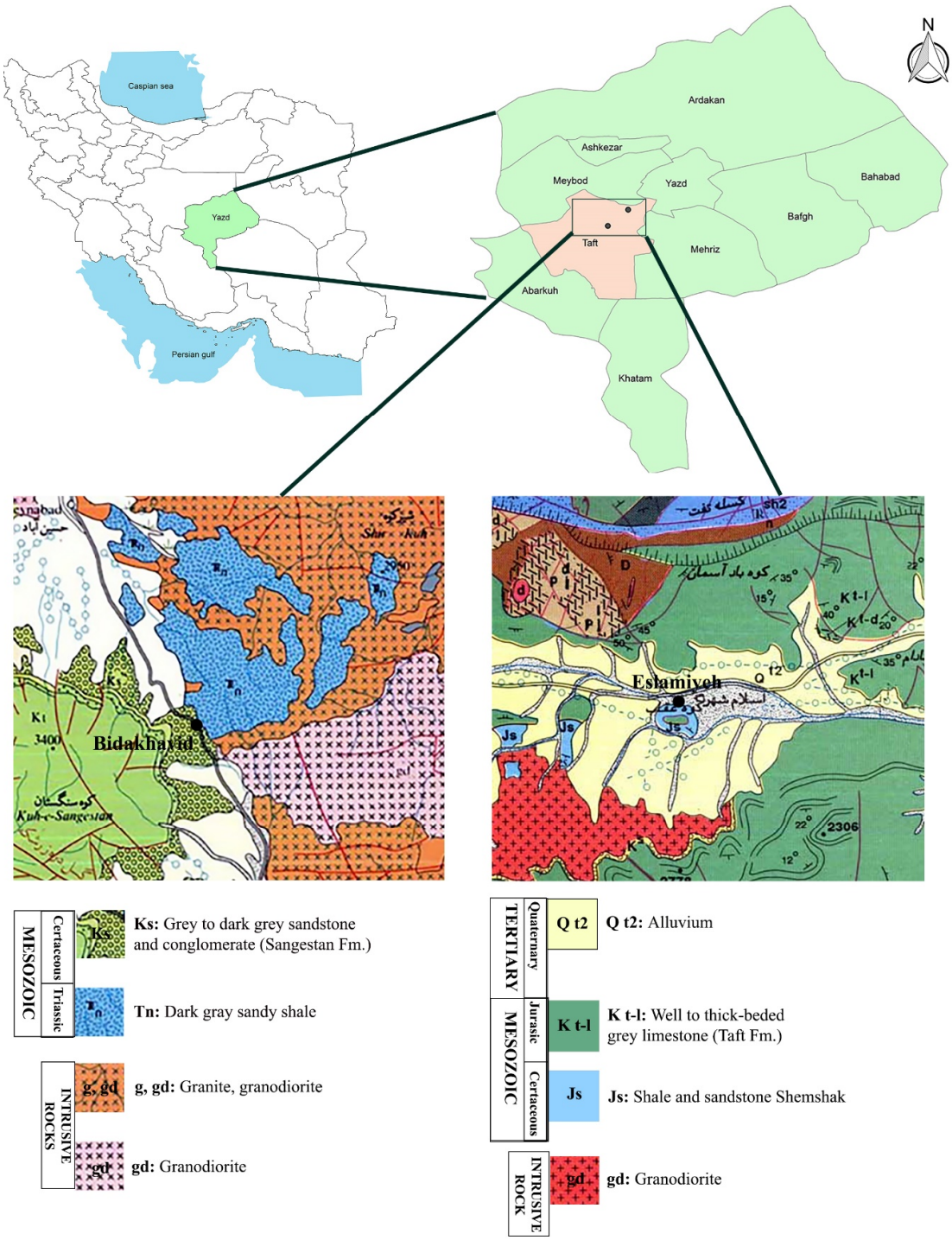

Figure 1. Geological map of the Bidakhavid and Eslamiyeh in Yazd province.

2.2. Petrography

The samples collected from the area can be divided into two categories: fine-grained sandstone and coarse-grained sandstone. The cross-section of the fine-grained sandstone (shown in Figure 2) displays laminations that vary in thickness. The mineralogy of this sample is composed of elongated Muscovite and quartz grains, along with a possible presence of clay minerals. The coarse-grained sandstone (also shown in Figure 2) contains clear quartz, slightly weathered feldspars, and pebbles. The presence of feldspar indicates a dry climate in the region that prevented it from decomposing. The sedimentation process in this area was also intense, which further explains the

abundance of feldspar in the rock texture. The presence of unrounded and angular quartz and feldspar in the samples suggests minimal block movement and proximity to the origin. A small amount of biotite and a lesser percentage of mica can also be observed in some of the samples from this area. The average grain size of the fine-grained sandstone was measured to be around 0.7 mm at the limit of silt in the medium and coarse sections. The X-ray diffraction (XRD) analysis results confirmed the minerals identified in the petrographic examination of the thin sections under a microscope. Tables 1 and 2 and Figures 3 and 4 demonstrate that the composition of the two samples is relatively similar, with the main difference being in their grain sizes.

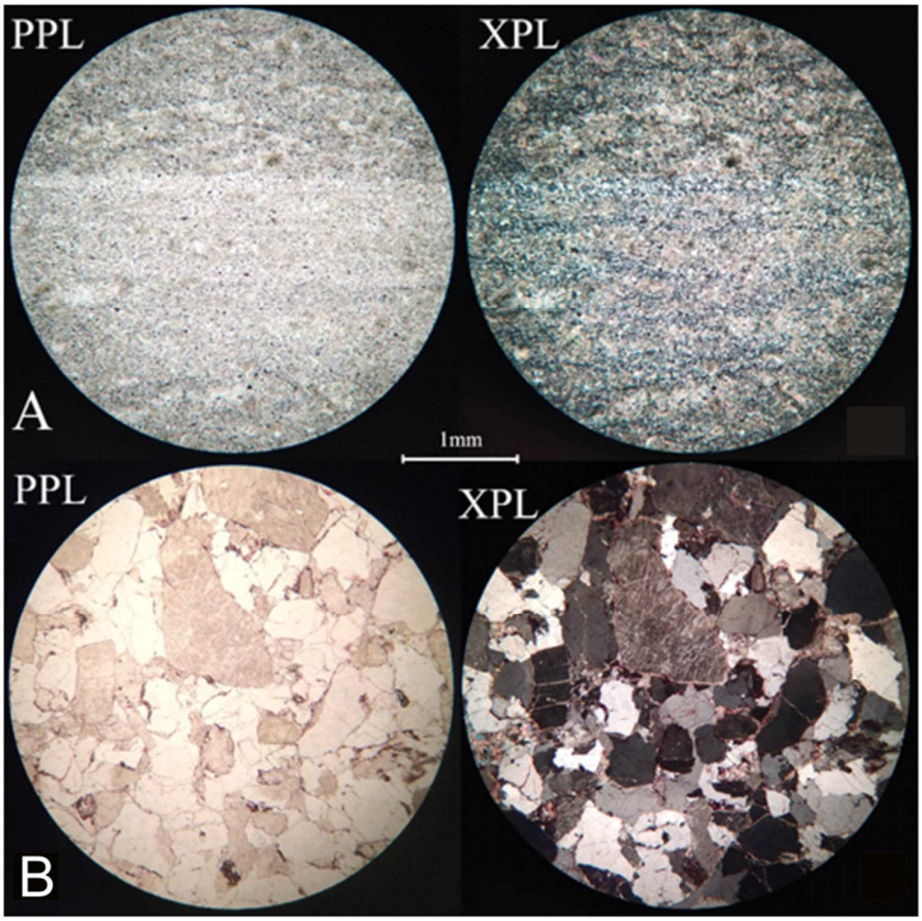

Figure 2. Samples A: Fine-grained sandstone, Samples B: Coarse-grained sandstone.

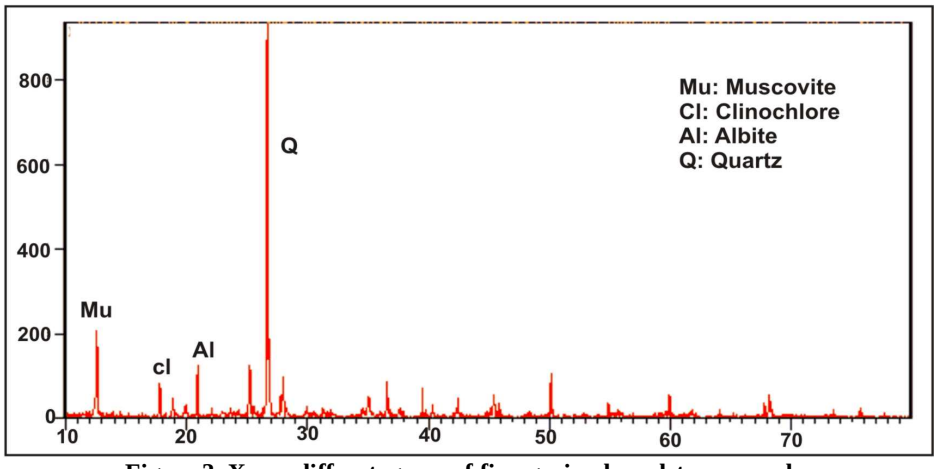

Figure 3. X-ray diffractogram of fine-grained sandstone sample.

Table 1. Results of XRD analysis of fine-grained sandstone samples.

Ref. code	Score	Scale factor	Chemical formula	Mineral name
96-500-0036	45	0.534	$Si_{3.00}O_{6.00}$	Quartz
96-900-1633	22	0.075	$Na_{2.00}Al_{2.00}Si_{6.00}O_{16.00}$	Albite
96-900-4643	21	0.099	$O_{46.88}F_{1.12}Na_{0.56}Rb_{0.08}K_{3.36}Si_{12.77}Al_{10.27}Fe_{0.52}Li_{0.52}Mg_{0.04}$	Muscovite
96-901-0131	13	0.098	$Mg_{4.50}Fe_{0.50}Al_{1.84}Si_{3.16}O_{18.00}$	Clinochlore

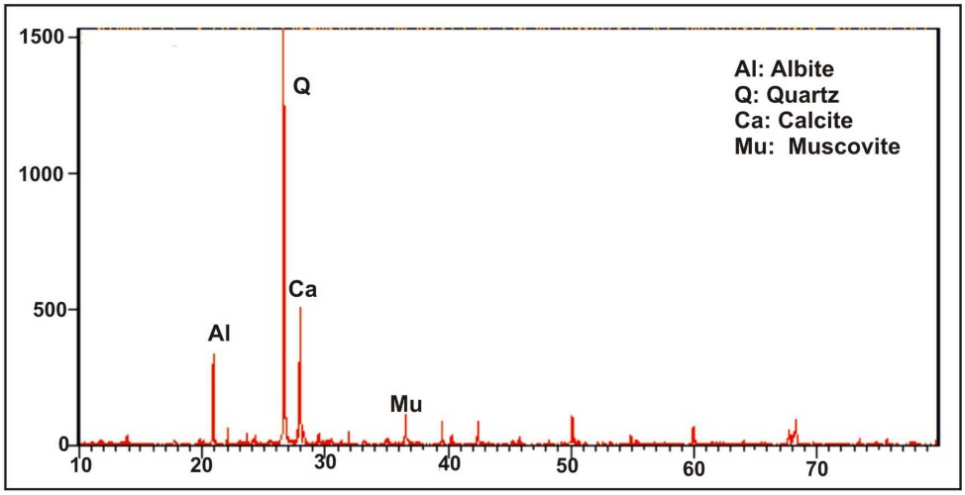

Figure 4. X-ray diffractogram of coarse-grain sandstone sample.

Table 2. Results of XRD analysis of coarse-grain sandstone samples.

Ref. code	Score	Scale factor	Chemical formula	Mineral name
96-500-0036	49	0.955	$Si_{3.00}O_{6.00}$	Quartz
96-900-1632	35	0.189	$Na_{2.00}Al_{2.00}Si_{6.00}O_{16.00}$	Albite
96-901-6707	23	0.031	$Ca_{6.00}C_{6.00}O_{18.00}$	Calcite
96-901-4961	9	0.038	$K_{3.44}Na_{0.40}Al_{11.60}Fe_{0.16}Mg_{0.24}Si_{12.00}O_{48.00}$	Muscovite

2.2. Uniaxial compressive strength test

In the recent study, six samples were subjected to uniaxial loading after preparation according to the American Society for Testing and Materials (ASTM) D 2938 [45] standard, which are shown in Figure 5. The geometric characteristics of these samples are presented in Table 3. The numbers of the samples that start with the letter E are related to the Eslamiyeh region, and the codes that start with the letter B are taken from the Bidakhavid region. The results of these tests are summarized in Table 4. The elasticity modulus (E) of rock is an important and influential parameter in the analysis and modeling of rock structures as well as the fracture in the rock mass. This parameter is directly effective in determining the amount of elastic deformation of walls and underground spaces. Therefore, it is necessary to evaluate its values at the beginning of any project. There are three methods to calculate the modulus of elasticity. These three methods give three different values of secant modulus, average modulus and tangent modulus. In this study, the tangent modulus is estimated by drawing a tangent line to the 50% point of compressive strength. The cracking pattern in uniaxial compressive strength (UCS) refers to the pattern of micro-cracks that form in a material when it is subjected to a uniaxial compressive load. UCS is a measure of the maximum compression that a material can withstand without undergoing permanent deformation. When a material is subjected to a uniaxial compressive load, it undergoes a series of deformation processes that lead to the formation of micro-cracks. These micro-cracks can develop into larger cracks, and eventually lead to material failure. The cracking pattern in UCS can vary depending on the properties of the material being tested and the loading conditions. The cracking pattern in UCS can provide important information about the properties of the material being tested. For example, the alignment of the cracks can provide information about the anisotropic properties of the material. Additionally, the size and distribution of the cracks can provide information about the

material's toughness and ductility. Understanding the cracking pattern can also help engineers design structures and materials that can withstand compressive loads more effectively. Figure5 shows two mode of cracking mode-I (Tension cracks) and mode-II (shear cracks) for the both coarse grain sandstone and fine grain sandstone.

Table 3. Geometric characteristics of uniaxial compressive strength test samples.

Sample ID	Thickness (mm)	Length (mm)
E-1-3	52.9	106.4
E-2-3	51.57	111.2
E-3-3	51.7	105
B-1-6	52	116
B-2-6	52.25	112
B-3-6	51.55	116.5

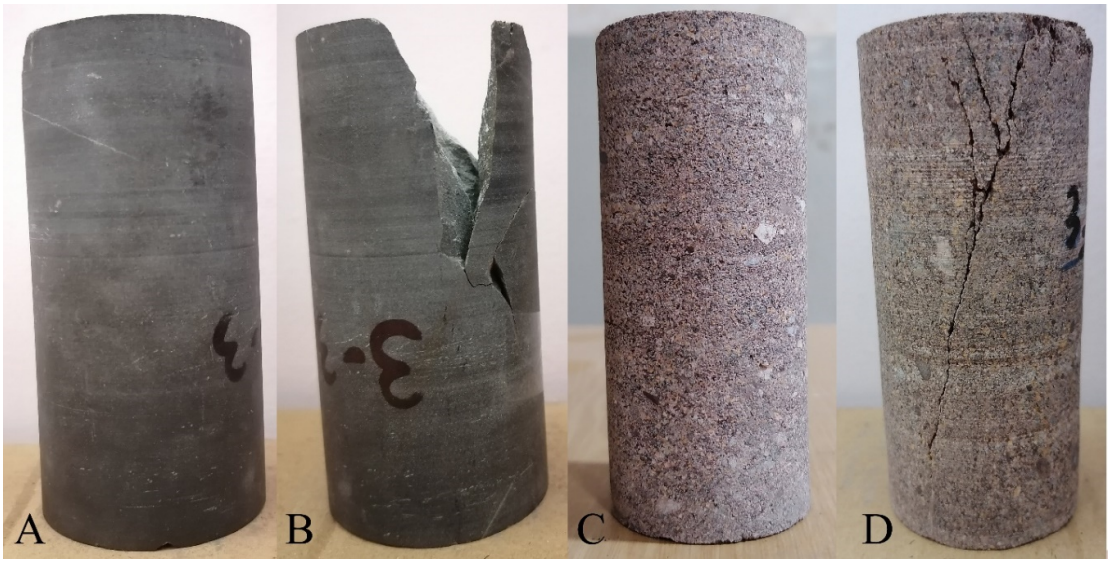

Figure 5. UCS tests, A and B: fine-grained sandstone samples, C and D: coarse-grained sandstone samples.

Table 4. Uniaxial compressive strength test results of fine-grained and coarse-grained sandstone samples.

Sample ID	Uniaxial compressive strength (MPa)	Average modulus of elasticity (50% tangent) (GPa)
E-1-3	98.14	12.8
E-2-3	62.34	11.9
E-3-3	85.31	13.3
B-1-6	32.87	4.6
B-2-6	31.16	4.2
B-3-6	25.35	4.7

2.3. Brazilian test

This test was developed to indirectly measure the uniaxial tensile strength of the rock sample. Loading the force on the rock sample eventually causes it to break. If the stresses applied to the rock are of tensile type, tensile ruptures and if they are compressive, ruptures related to pressure (shearing) occur in the rock. Generally, the resistance of rocks against tension is less than its pressure, and they break under less load than its pressure. Tensile strength is the maximum tensile stress that a material can withstand until it breaks. The Brazilian test is based on the experiment that by applying diagonal pressure to cylindrical rock samples, the induced tensile stress spreads along the perpendicular to the loading axis, and when this stress exceeds the tensile strength of the rock, the sample breaks (Figure 6).

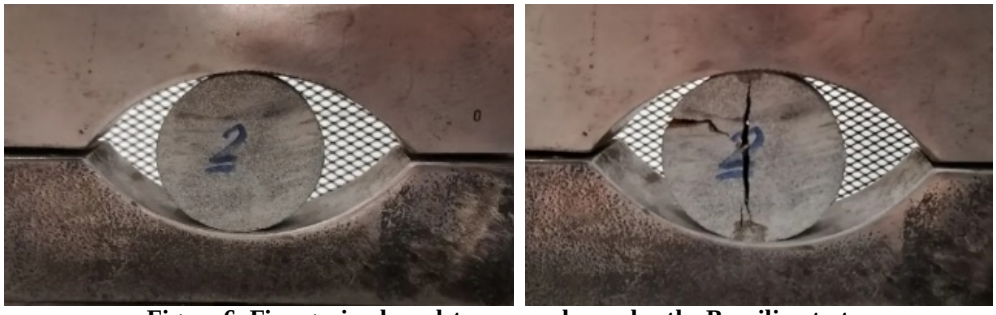

Figure 6. Fine-grained sandstone samples under the Brazilian test.

In the Brazilian test, disc-shaped samples with a ratio of length to diameter equal to 0.5 mm to 0.75 mm are placed in the standard loading jaw with curvature. Then loading at a constant rate is applied to the sample. In standard tests, the sample is often broken within 15-30 seconds, and the axial force is read at the moment of breaking. The standard failure pattern in this test will be diagonal and in the direction of applying pressure. By measuring the applied load at the moment of rupture, it is possible to calculate the tensile strength from Equation 1.

$$\sigma_t = (2/\pi) \times \left(\frac{P}{D} \times t\right) (MPa) \quad (1)$$

where:

σ_t is the tensile strength of the sample (MPa)

P is the load at the moment of breaking (N)

D is the diameter of the sample (mm)

t is the thickness of the sample in the center (mm)

In the recent study, six Brazilian tests of two rock samples have been subjected to the Brazilian test after preparation according to the standard of the International Association of Rock Mechanics (ISRM)[46]. Table 5 shows the geometric characteristics of the samples. The results of Brazilian test of sandstone samples are summarized in Table 6.

Table 5. Geometric characteristics of Brazilian test samples.

Sample ID	Diameter (mm)	Thickness (mm)
E-1-3	53	25
E-2-3	53	25
B-1-6	52	24.5
B-2-6	52	34.5
B-3-6	52.15	35.5
B-4-6	52	30.5

Table 6. Brazilian test results for fine and coarse-grain sandstone samples.

Sample ID	Force (kN)	Tensile strength of sample (MPa)
E-1-3	22.5	10.8
E-2-3	17.1	8.22
B-1-6	3.6	1.8
B-2-6	6.1	2.17
B-3-6	6	2.06
B-4-6	5.3	2.13

3. Numerical Modeling

Numerical modeling has been used to investigate the effect of grain size on the mechanical behavior of sandstone in laboratory scale. In this research work, the numerical model is based on the distinct element method (DEM) with particle flow code (PFC) is a more practical and robust method for modeling fracture initiation and propagation under complex stress conditions [47]. However, it is difficult to reveal its mechanical behavior by laboratory experiments. Hence, the numerical modeling in PFC shows the failure mechanism at the microscopic level. In this study, ten models were given for modeling the uniaxial compressive strength test, and the grain size was increased from 0.08 to 0.9 mm. For the indirect tensile strength test (Brazilian), four models in different dimensions have been examined.

3.1. Calibration of micro-parameters

Calibration of micro-parameters with macro-parameters is an essential part of numerical modeling. However, in PFC2D, it is difficult to obtain the microscopic parameters experimentally. PFC modeling has been used to correlate the microscopic and macroscopic properties of rocks. However, the highly non-linear behavior of particle interactions may lead to suboptimal microscopic parameters. Trial-error method is the best method to obtain more appropriate and reasonable micro-parameters by fitting macro-mechanical properties [48-51]. This section aims to assess the validity of the numerical modeling results by examining the stress-strain curve and the peak strength value of the microscopic properties, which are presented in Figures 7 and 8. The trial-error method was utilized to ensure that the numerical results align with the experimental results. This iterative process was repeated until a reasonable correlation between the numerical, and experimental results were achieved. The outcome of this study demonstrates that the numerical modeling results were consistent with the experimental results, which further strengthens the credibility and reliability of the modeling methodology employed.

In the built models, the mechanical properties of the grains are considered the same as shown in Table 7. The flat joint model (FJM) has been applied for the numerical modeling in PFC. It is worth noting that the effective porosity is assumed to be zero due to its insignificance. In this section, to validate the flat joint model, a series of Brazilian tests were conducted on fine-grained sandstone samples (Figure 9). The model is compared and verified with the pattern failure mechanism. Standard Brazilian test specimens were prepared to study the mechanical behavior. In addition, a reasonable agreement between the Flat joint model in PFC2D and the failure mechanism model in the Brazilian test is obtained (Figure 10).

Table 7. Micro-mechanical properties of grains in the FJM model.

Mechanical properties	Value
Particle density (kg/m^3)	2550
Young's modulus of the flat joint bond (GPa)	0.6
Ratio of normal to shear stiffness of the flat joint bond	0.1
Particle friction coefficient	0.7
Flat joint bond tensile strength (Pa)	6.8×10^6
Flat joint bond cohesion (Pa)	150×10^5
Friction angle (degree)	15

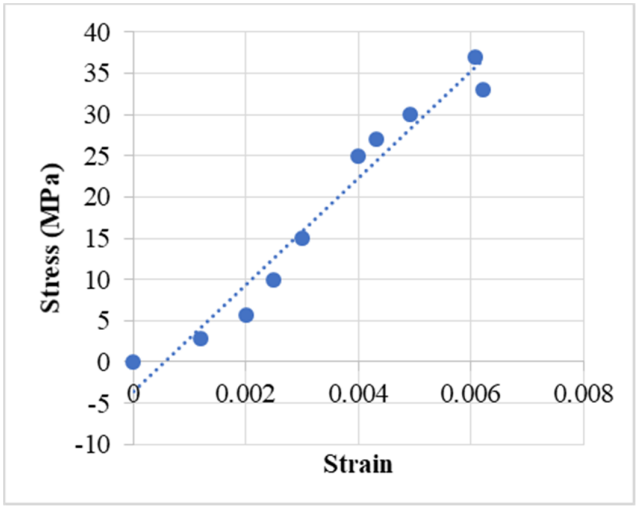

Figure 7. Stress-strain curve obtained from UCS test.

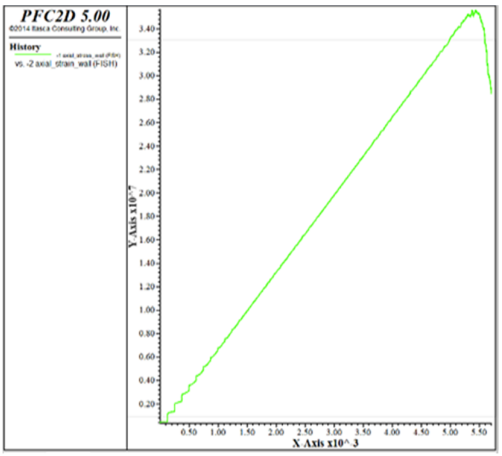

Figure 8. Stress-strain curve obtained from the calibrated numerical model.

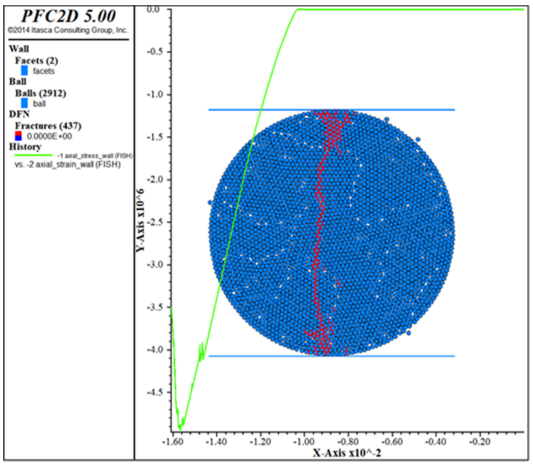

Figure 9. Failure pattern of fine-grained sandstone sample in Brazilian test.

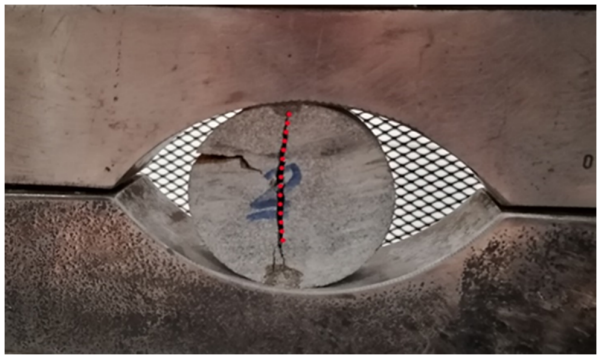

Figure 10. Failure pattern of Brazilian test sample in numerical model.

3.2. Results of numerical modeling

The flat joint model (FJM) is a granular model with an average grain size of 0.3 to 0.5 mm to match the laboratory response of coarse-grained and fine-grained sandstone (Figure 11). The grain size in the model is close to the average grain size of sandstone. In order to analyze the compressive strength and tensile strength results, the model with the same properties and variable dimensions is considered.

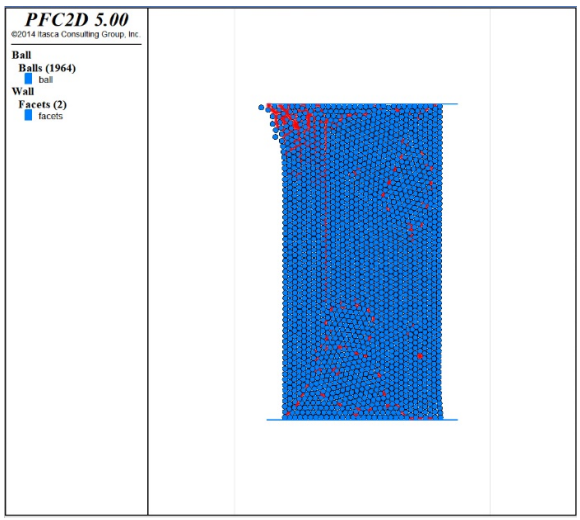

Figure 11. A sample of uniaxial compressive strength test modeling.

The effect of sample size on rock strength has been widely discussed in the literature, and it is generally accepted that there is a significant decrease in strength as sample size increases. Hoek and Brown [52] proposed the following empirical relationship of Equation 2.

$$\sigma_{cd} = \sigma_{c50}(50/d)^{0.18} \quad (2)$$

where:

σ_{cd} is the uniaxial compressive strength relates a rock sample of diameter d (mm)

σ_{c50} of a 50 mm diameter

d is the diameter (mm)

They concluded that the reduction in strength was attributed to greater opportunity for failure through pre-existing grain surrounds and micro-cracks. By increasing the sample size, more defects can be included in the test sample, which helps to reduce the resistance. This relationship also shows that when a large number of defects are included in the sample, the resistance may reach a constant value. This corresponds to the representative elementary volume (REV), which is defined as the minimum sample size at which test results are independent of size. Table 8 shows the dimensions of the grains of the compressive strength model, which shows the effect of grain dimensions on the compressive strength in Figure 12 that the reduction of the grain size leads to the reduction of the compressive strength.

Table 8. Dimensions of grains calibration with uniaxial compressive strength.

Grain size (mm)	Compressive strength (MPa)
0.08	36.4
0.09	36.2
0.1	36.1
0.2	35.8
0.4	35.6
0.5	35.6
0.6	34.8
0.7	34.7
0.8	34
0.9	33.8

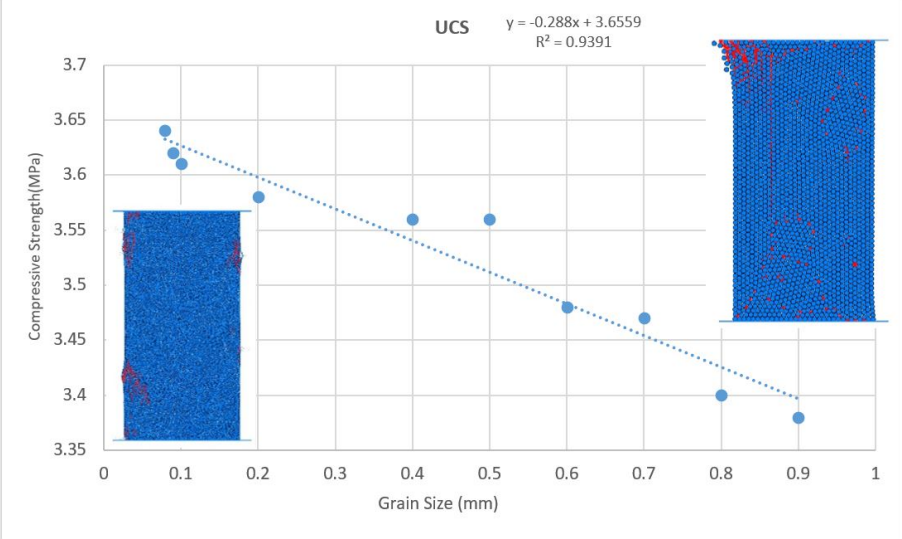

Figure 12. Trending of compressive strength with increasing grain size in UCS test.

In the Brazilian test, modeling was used to improve the problems related to sample preparation and direct stress testing. The compressive load causes normal tensile stresses along the vertical loading diameter. The maximum tensile stress obtained is considered as the indirect tensile strength of the rock. Hondros [53] proposed a set of relations to determine the complete stress distribution in a Brazilian disc. These equations showed that the maximum tensile stress occurs under the loading diameter and then the indirect tensile strength can be calculated by the given Equation 3.

$$\sigma_t = \frac{P}{\pi r t} \quad (3)$$

where:

P is the breaking load (N)

r is the radius of the disk (mm)

t is the thickness of the disk (mm)

According to the Griffiths criterion, the center of the Brazilian test disc is the crack initiation point where conditions for tensile failure are first established. Heterogeneity plays an important role in the overall behavior of the disc during the Brazilian test. It should also be noted that in addition to the effect of grain size, other characteristics such as inter grain connection, intensity of micro-cracks, and orientation also contribute to the ultimate strength of the Brazilian test. The tensile strength obtained from the numerical simulations, as shown in Figure 13, shows that the indirect tensile strength decreases with increasing grain dimensions.

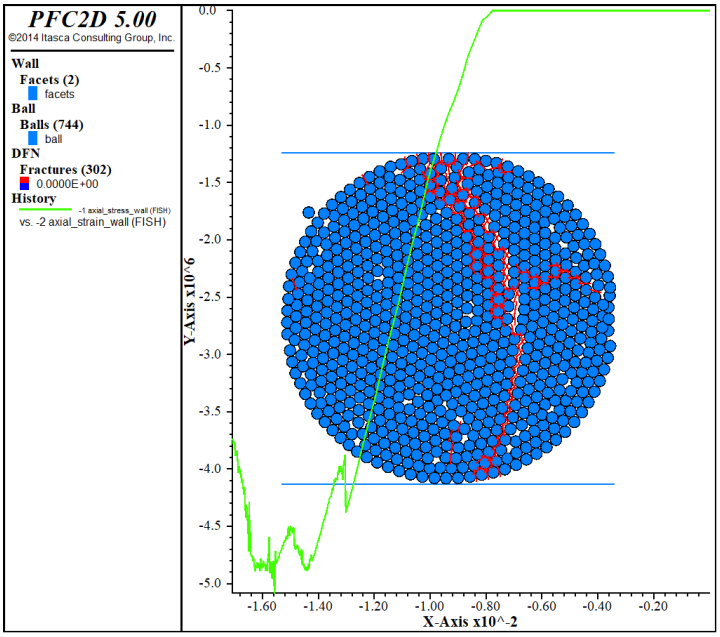

Figure 13. A sample of the Brazilian test modeling along with the stress-strain curve.

Table 9. Dimensions of the grain size calibration with the Brazilian test.

Grain size (mm)	Tensile strength (MPa)
0.3	12
0.4	6.2
0.8	5
1	5.1

The area under the stress-strain curve of the rock before the ultimate strength is an indicator of energy absorption and depends on the ultimate strength and modulus of elasticity. The modulus of elasticity has a significant effect on rock deformation and fracture, while it is not considered as an effective parameter in rock brittleness calculations. Brittle rock failure begins with the loss of cohesion (cement) between grains in the early stages, followed by the expansion and mobility of frictional resistance [54]. In the rock sample, behavioral changes start from 30% to 50% during the peak stress, and crack formation continues from 70% to 85% during the highest stress. Crack propagation in brittle materials, for example rock, is entirely dependent on elastic energy. In fracture mechanics, elastic energy is the basic and necessary energy for crack propagation. Irwin [55] provided a flexible solution of the energy required to initiate a crack at a crack tip, and showed that if the plastic area across the crack tip is minimal compared to the length of the crack, it does not depend on the stress state. Crack propagation is strongly dependent on fracture toughness mode-II, but direct estimation of rock fracture toughness is difficult due to the limited number of available cores and long-term consumption [56]. The numerical analysis method showed that the dominant failure mode is tensile, regardless of the shear stage [57]. In rock materials, due to heterogeneity, porosity, bedding plane, etc., fracture toughness data is scattered, and a small number of samples cannot provide versatile and reliable data. In this study, to check the modulus of

elasticity, the stress and strain data related to the modeling of the uniaxial compressive strength test and the dimensions mentioned in Table 10 were used and the modulus of elasticity was calculated. As can be seen from the Figure 15, with the increase in the dimensions of the grains, the modulus of elasticity shows a decreasing trend. The validated trial and error method were applied to all UCS test samples, as illustrated in Figure 16.

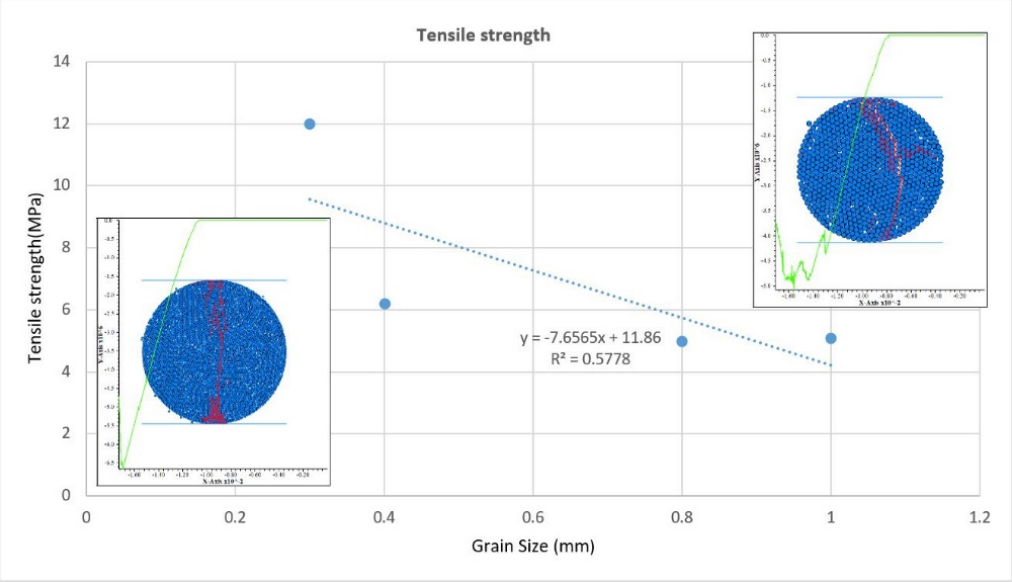

Figure 14. Tensile strength decreasing with increasing grain size in Brazilian test.

Table 10. Dimensions of the grains used in the calibration of the modulus of elasticity.

Grain size (mm)	Elasticity modulus (GPa)
0.08	0.654
0.09	0.659
0.1	0.662
0.2	0.655
0.4	0.629
0.6	0.644
0.7	0.625
0.8	0.633
0.9	0.619

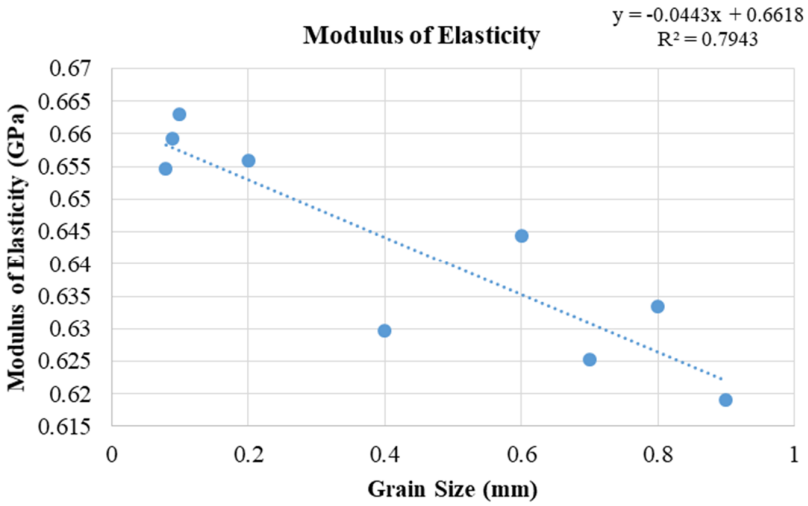

Figure 15. Trend of elasticity modulus changes with grain size.

Figure 16. Trial-error method validation of UCS tests in PFC.

4. Conclusions

The results obtained from changes in macroscopic properties have all been expected, because as the dimensions of the grains become smaller, the amount of contact surface will increase and this factor will increase the intergranular resistance and increase the resistance properties of the sandstone.

- The compressive strength of the rock material decreases with the increase in the size of the grains. The correlation coefficient $R^2 = 0.9391$ has been obtained, which shows a positive relationship between the dimensions of the grains and the compressive strength.
- The tensile strength of the rock material also decreases with the increase in the dimensions of

the grains, and the correlation coefficient in this case is $R^2 = 0.57$. As the dimensions of the grains increase, the modulus of elasticity decreases. In this case, the correlation coefficient $R^2 = 0.79$ has been obtained.

- The results showed that all three investigated macroscopic properties including compressive strength, tensile strength and modulus of elasticity; it decreases with the increase of grain size, with the difference that the effect of changes in compressive strength caused by the change of grain size was greater.
- The amount of tensile strength in the Brazilian test did not change significantly in the dimensions of grains below 0.2 (including 0.08 and 0.09) and for this reason, it was removed from the graph.

References

[1]. Sultan Shah, K., Mohd Hashim, M.H.B., Rehman, H.U., and Ariffin, K.S.B. (2022). Evaluating microscale failure response of various weathering grade sandstones based on micro-scale observation and micro-structural modelling subjected to wet and dry cycles. Journal of Mining and Environment, 13 (2): 341-355.

[2]. Shah, K.S., Mohd Hashim, M.H., Rehman, H., and Ariffin, K.S. (2021). Application of Stochastic Simulation in Assessing Effect of Particle Morphology on Fracture Characteristics of Sandstone. Journal of Mining and Environment, 12(4): 969-986.

[3]. Fattahi, H. (2020). A New Method for Predicting Indirect Tensile Strength of Sandstone Rock Samples. Journal of Mining and Environment, 11(3): 899-908.

[4]. Shah, K.S., Mohd Hashim, M.H., and Ariffin, K.S. (2021). Monte Carlo Simulation-based Uncertainty Integration into Rock Particle Shape Descriptor Distributions. Journal of Mining and Environment, 12 (2): 299-311.

[5]. Golewski, G.L. (2023). Combined Effect of Coal Fly Ash (CFA) and Nanosilica (nS) on the Strength Parameters and Microstructural Properties of Eco-Friendly Concrete. Energies, 16 (1): 452.

[6]. Golewski, G.L. and Szostak, B. (2022). Strength and microstructure of composites with cement matrixes modified by fly ash and active seeds of CSH phase. Structural Engineering and Mechanics, 82 (4): 543-556.

[7]. Golewski, G.L. (2022). An extensive investigations on fracture parameters of concretes based on quaternary binders (QBC) by means of the DIC technique. Construction and Building Materials, 351, 128823.

[8]. Wang, J., Song, Z., Zhao, B., Liu, X., Liu, J., and Lai, J. (2018). A study on the mechanical behavior and statistical damage constitutive model of sandstone. Arabian Journal for Science and Engineering, 43, 5179-5192.

[9]. Hosseini, M. and Khodayari, A.R. (2019). Effect of freeze-thaw cycle on strength and rock strength parameters (A Lushan sandstone case study). Journal of Mining and Environment, 10 (1): 257-270.

[10]. Utili, S. and Nova, R.O.B.E.R.T.O. (2008). DEM analysis of bonded granular geomaterials. International Journal for Numerical and Analytical Methods in Geomechanics, 32 (17): 1997-2031.

[11]. Ding, X., Zhang, L., Zhu, H., and Zhang, Q. (2014). Effect of model scale and particle size distribution on PFC3D simulation results. Rock mechanics and rock engineering, 47, 2139-2156.

[12]. Nemat-Nasser, S. (1986). Overall stresses and strains in solids with microstructure. Modelling Small Deformations of Polycrystals, 41-64.

[13]. Külekçi, G., Vural, A., and Aliyazıcıoğlu, Ş. (2022). Assessment of Excavability Classification in A Limestone Quarry: A Case Study from Bayburt, Türkiye. Iranian Journal of Earth Sciences. 14 (4).

[14]. Kulekci, G., Yilmaz, A. O., and Cullu, M. (2021). Experimental investigation of usability of construction waste as aggregate. Journal of Mining and Environment, 12 (1): 63-76.

[15]. Kahraman, S.A.İ.R. and Alber, M. (2008). Triaxial strength of a fault breccia of weak rocks in a strong matrix. Bulletin of engineering geology and the environment, 67, 435-441.

[16]. Amann, F., Kaiser, P., and Button, E.A. (2012). Experimental study of brittle behavior of clay shale in rapid triaxial compression. Rock Mechanics and Rock Engineering, 45, 21-33.

[17]. Zhang, Y., Shao, J.F., Xu, W.Y., Zhao, H.B., and Wang, W. (2015). Experimental and numerical investigations on strength and deformation behavior of cataclastic sandstone. Rock Mechanics and Rock Engineering, 48, 1083-1096.

[18]. Cundall, P. A., Potyondy, D. O., and Lee, C. A. (1996, September). Micromechanics-based models for fracture and breakout around the mine-by tunnel. In proceedings, international conference on deep geological disposal of radioactive waste, Winnipeg. Edited by JB Martino and CD Martin. Canadian Nuclear Society, Toronto (pp. 113-122).

[19]. Hazzard, J.F. and Young, R.P. (2000). Simulating acoustic emissions in bonded-particle models of rock. International Journal of Rock Mechanics and Mining Sciences, 37 (5): 867-872.

[20]. Fakhimi, A., Carvalho, F., Ishida, T., and Labuz, J. F. (2002). Simulation of failure around a circular opening in rock. International Journal of Rock Mechanics and Mining Sciences, 39 (4): 507-515.

[21]. Diederichs, M.S. (2003). Manuel rocha medal recipient rock fracture and collapse under low confinement conditions. Rock Mechanics and Rock Engineering, 36, 339-381.

[22]. Hazzard, J.F. and Young, R. P. (2004). Dynamic modelling of induced seismicity. International journal of rock mechanics and mining sciences, 41 (8): 1365-1376.

[23]. Fakhimi, A., Riedel, J.J., and Labuz, J.F. (2006). Shear banding in sandstone: Physical and numerical studies. International Journal of Geomechanics, 6 (3): 185-194.

[24]. Wanne, T.S. and Young, R.P. (2008). Bonded-particle modeling of thermally fractured granite. International Journal of Rock mechanics and mining Sciences, 45 (5): 789-799.

[25]. Zhao, Z. (2013). Gouge particle evolution in a rock fracture undergoing shear: a microscopic DEM study. Rock Mechanics and Rock Engineering, 46, 1461-1479.

[26]. Khazaei, C., Hazzard, J., and Chalaturnyk, R. (2015). Damage quantification of intact rocks using acoustic emission energies recorded during uniaxial compression test and discrete element modeling. Computers and Geotechnics, 67, 94-102.

[27]. Ozturk, H. and Altinpinar, M. (2017). The estimation of uniaxial compressive strength conversion factor of trona and interbeds from point load tests and numerical modeling. Journal of African Earth Sciences, 131, 71-79.

[28]. He, J. and Afolagboye, L. O. (2018). Influence of layer orientation and interlayer bonding force on the mechanical behavior of shale under Brazilian test conditions. Acta Mechanica Sinica, 34, 349-358.

[29]. Yin, P.F. and Yang, S.Q. (2019). Discrete element modeling of strength and failure behavior of transversely isotropic rock under uniaxial compression. Journal of the Geological Society of India, 93, 235-246.

[30]. Zhou, C., Karakus, M., Xu, C., and Shen, J. (2020). A new damage model accounting the effect of joint orientation for the jointed rock mass. Arabian Journal of Geosciences, 13, 1-13.

[31]. Bahaaddini, M., Hagan, P.C., Mitra, R., and Hebblewhite, B.K. (2015). Parametric study of smooth joint parameters on the shear behaviour of rock joints. Rock Mechanics and Rock Engineering, 48, 923-940.

[32]. Zhao, W., Huang, R., and Yan, M. (2015). Study on the deformation and failure modes of rock mass containing concentrated parallel joints with different spacing and number based on smooth joint model in PFC. Arabian journal of geosciences, 8, 7887-7897.

[33]. Huang, D., Wang, J., and Liu, S. (2015). A comprehensive study on the smooth joint model in DEM simulation of jointed rock masses. Granular Matter, 17, 775-791.

[34]. Wang, T., Xu, D., Elsworth, D., and Zhou, W. (2016). Distinct element modeling of strength variation in jointed rock masses under uniaxial compression. Geomechanics and Geophysics for Geo-Energy and Geo-Resources, 2, 11-24.

[35]. Chong, Z., Li, X., Hou, P., Wu, Y., Zhang, J., Chen, T., and Liang, S. (2017). Numerical investigation of bedding plane parameters of transversely isotropic shale. Rock Mechanics and Rock Engineering, 50, 1183-1204.

[36]. Chong, Z., Li, X., and Hou, P. (2019). Experimental and numerical study of the effects of layer orientation on the mechanical behavior of shale. Arabian Journal for Science and Engineering, 44, 4725-4743.

[37]. Huan, J. Y., He, M. M., Zhang, Z. Q., and Li, N. (2020). Parametric study of integrity on the mechanical properties of transversely isotropic rock mass using DEM. Bulletin of Engineering Geology and the Environment, 79, 2005-2020.

[38]. Lei, B., Li, H., Zuo, J., Liu, H., Yu, M., and Wu, G. (2021). Meso-fracture mechanism of Longmaxi shale with different crack-depth ratios: experimental and numerical investigations. Engineering Fracture Mechanics, 257, 108025.

[39]. Ghorbani, M. (2013). The economic geology of Iran. Mineral deposits and natural resources. Springer, 1-450.

[40]. Ghorbani, M. (2021). The geology of Iran: tectonic, magmatism and metamorphism. Springer International Publishing.

[41]. Emami Meybodi, E. and Jalali, S. M. E. (2015). Estimation of Fragmentation on Geometrical Viewpoint. Journal of Analytical and Numerical Methods in Mining Engineering, 5 (9): 51-61.

[42]. Ghorbani, M. (2019). Lithostratigraphy of Iran (p. 274). Cham: Springer.

[43]. Emami Meybodi, E., Hajibagheri Foroshani, J., and Kargaran Bafghi, F. (2022). Numerical modeling for Selection of appropriate tunneling method in S station of Isfahan subway. 11 (29): 27-40.

[44]. Meybodi, E. E., Hussain, S. K., Torabi-Kaveh, M., and Ali, S. (2022). Role of karstic features in instability of the wall of an open-pit mine (case study: Sadat Sirize Iron Mine, Iran). Carbonates and Evaporites, 37 (3): 52.

[45]. ASTM, D. (1995). 2938, Standard test method for unconfined compressive strength of intact rock core specimens. ASTM International, West Conshohocken, PA.

[46]. Bieniawski, Z.T., and Hawkes, I. (1978). Suggested methods for determining tensile strength of rock materials. International Journal of Rock Mechanics and Mining Sciences, 15 (3): 99-103.

[47]. Pirhooshyaran, M. R. and Nikkhah, M. (2022). Hydraulic fracture patterns in fractured rock mass using coupled hydromechanical modeling in the bonded particle model. Modeling Earth Systems and Environment, 1-14.

[48]. Emami Meybodi, E., Hussain, S. K., Fatehi Marji, M., and Rasouli, V. (2022). Application of Machine Learning Models for Predicting Rock Fracture Toughness Mode-I and Mode-II. Journal of Mining and Environment, 13 (2): 465-480.

[49]. Yang, S. Q., Tian, W. L., Huang, Y. H., Ranjith, P. G., and Ju, Y. (2016). An experimental and numerical study on cracking behavior of brittle sandstone containing two non-coplanar fissures under uniaxial compression. Rock Mechanics and Rock Engineering, 49, 1497-1515.

[50]. Emami Meybodi, E., Hussain, S. K., and Fatehi Marji, M. (2023). Experimental Evaluation and Discrete Element Modeling of Shale Delamination Mechanism. Journal of Mining and Environment, 14 (1): 259-276.

[51]. Emami Meybodi, E., DastBaravarde, A., Hussain, S. K., and Karimdost, S. (2023). Machine-learning method applied to provide the best predictive model for rock mass deformability modulus (E m). Environmental Earth Sciences, 82 (6): 149.

[52]. Brown, E. T. and Hoek, E. (1980). Underground excavations in rock. CRC Press.

[53]. Hondros, G. (1959). The evaluation of Poisson's ratio and the modulus of materials of a low tensile resistance by the Brazilian (indirect tensile) test with particular reference to concrete. Aust. J. Appl. Sci., 10, 243-264.

[54]. Barton, N. (2013). Shear strength criteria for rock, rock joints, rockfill and rock masses: Problems and some solutions. Journal of Rock Mechanics and Geotechnical Engineering, 5 (4): 249-261.

[55]. Irwin, G.R. (1957). Analysis of stresses and strains near the end of a crack traversing a plate.

[56]. Jin, Y., Yuan, J., Chen, M., Chen, K. P., Lu, Y., and Wang, H. (2011). Determination of rock fracture toughness K IIC and its relationship with tensile strength. Rock mechanics and rock engineering, 44, 621-627.

[57]. Sun, W., Du, H., Zhou, F., and Shao, J. (2019). Experimental study of crack propagation of rock-like specimens containing conjugate fractures. Geomechanics and Engineering, 17 (4): 323-331.

تجزیه و تحلیل اثر اندازه دانه بر خواص مکانیکی ماسه سنگ با روش‌های تجربی و عددی

عنایت الله امامی میبدی* و فاطمه تعجبیان

گروه زمین شناسی، دانشگاه یزد، یزد، ایران

ارسال 2023/03/29، پذیرش 2023/05/05

* نویسنده مسئول مکاتبات: en.emami@yazd.ac.ir

چکیده:

با توجه به چالش یافتن نمونه‌های سنگی یکسان با اندازه‌های دانه‌های مختلف، بررسی تأثیر بافت بر مواد سنگ کمتر مورد توجه قرار گرفته است. با این حال، خواص ماکروسکوپی مانند مقاومت فشاری تک محوری، مقاومت کششی و مدول الاستیسیته می‌تواند نشان‌دهنده ویژگی‌های میکروسکوپی مانند خواص مقاومت بین دانه‌ای باشد که بر چقرمگی شکست سنگ تأثیر خواهد داشت. در این کار از هر دو روش تجربی و عددی برای بررسی اثر اندازه دانه بر خواص مکانیکی ماسه سنگ استفاده شده است. آزمون مقاومت فشاری تک محوری و آزمون کششی غیرمستقیم بر روی نمونه‌های ماسه‌سنگ با اندازه دانه‌های مختلف انجام شد. از نرم‌افزار کد جریان ذرات برای مدل‌سازی تأثیر ابعاد دانه بر خواص بین دانه‌ای استفاده گردید. از مدل اتصال مسطح در نرم‌افزار کد جریان ذرات استفاده شده است. هدف از این کار اعتبارسنجی مدل عددی بر اساس معیارهای مقاومت حداکثر و شکل منحنی تنش-کرنش برای تعیین اثر اندازه دانه بر رفتار مکانیکی سنگ است. نتایج نشان می‌دهد که افزایش اندازه دانه به طور معنی داری مقاومت فشاری، مقاومت کششی و مدول الاستیسیته را کاهش می‌دهد. تأثیر تغییر اندازه دانه بر مقاومت فشاری بیشتر از دو ویژگی دیگر است. ضریب همبستگی برای استحکام کششی و اندازه دانه $R^2 = 0.57$ است، در حالی که برای مدول الاستیسیته و اندازه دانه، $R^2 = 0.79$ است. نرم افزار PFC به کالیبراسیون خواص بین دانه‌ای و بررسی اثر تغییر اندازه دانه بر روی این خواص کمک می‌کند. به طور کلی، این مطالعه بینش‌های ارزشمندی را در مورد رابطه بین اندازه دانه و خواص مکانیکی ماسه سنگ ارائه می‌دهد که می‌تواند در کاربردهای مختلف مهندسی، به ویژه در ژئومکانیک نفت مفید باشد.

کلمات کلیدی: اندازه دانه، ماسه سنگ، PFC2D، روش اجزای گسسته، ویژگی های مکانیکی، FJM، UCS، تست برزیلی.